P-satI-D Shape Regulation of Soft Robots

Pustina, Pietro; Borja, Pablo; Santina, Cosimo Della; De Luca, Alessandro

DOI
10.1109/LRA.2022.3221304

Publication date
2023

Document Version
Final published version

Published in
IEEE Robotics and Automation Letters

Citation (APA)
Pustina, P., Borja, P., Santina, C. D., & De Luca, A. (2023). P-satI-D Shape Regulation of Soft Robots. *IEEE Robotics and Automation Letters*, *8*(1). https://doi.org/10.1109/LRA.2022.3221304

P-satI-D Shape Regulation of Soft Robots

Pietro Pustina, *Graduate Student Member, IEEE*, Pablo Borja, *Member, IEEE*, Cosimo Della Santina, *Member, IEEE*, and Alessandro De Luca, *Fellow, IEEE*

***Abstract*—Soft robots are intrinsically underactuated mechanical systems that operate under uncertainties and disturbances. In these conditions, this letter proposes two versions of PID-like control laws with a saturated integral action for the particularly challenging shape regulation task. The closed-loop system is asymptotically stabilized and matched constant disturbances are rejected using a very reduced amount of system information for control implementation. Stability is assessed on the underactuated dynamic model through the Invariant Set Theorem for two relevant classes of soft robots, i.e., elastically decoupled and elastically dominated soft robots. Extensive simulation results validate the proposed controllers.**

***Index Terms*—Control, and learning for soft robots, modeling, motion control, underactuated robots.**

I. Introduction

CONTINUUM soft robots are robotic systems made of continuously deformable materials [1]. Because of their compliant nature, soft robots have applications ranging from maintenance [2] to human rehabilitation [3]. In soft robotics, several open challenges need yet to be addressed, spanning from perception to control. These mainly stem from the infinite-dimensional nature of soft robots, whose dynamics is governed by nonlinear partial differential equations. To overcome this challenge, researchers have proposed approaches to obtain finite-dimensional but accurate descriptions of soft robots [4], [5], [6]. Several works, such as [7], [8], [9], have used finite-dimensional models for control purposes both in configuration and task space. Most of these new approaches build upon fully actuated approximations of the dynamics, which allow reconducting the control problem to standard rigid robot control theory. However, obtaining these simplified models implies relying on very coarse approximations. Developing model-based controllers this way has been a valuable heuristic to showcase the power of model-based controllers. Unfortunately, at the same time, using such rough approximations can lead to an erroneous assessment of stability and sub-optimal performance, which are essential features for systems that are supposed to interact with humans.

Therefore, a growing attention has been building around the topic of developing controllers for soft robots that operate outside the restrictive fully actuated framework. An early work dealing with this challenge is [10], which approximates the dynamics of soft robots as large-scale linear systems. This allows assessing that a control loop consisting of an observer and a controller derived from a reduced-order model can successfully stabilize the original dynamics. The architecture is validated experimentally. In [11], the authors propose an underactuated template model for the control design of soft robots. After studying the main system properties, they show how collocated and non-collocated feedback linearization asymptotically stabilize the arm in its unstable straight configuration. Also, [12] presents a controller for shape regulation of planar soft robots by matching the robot with an underactuated rigid-link model. Even if theoretically sound, these controllers have limited practical applicability as they have complex forms and are potentially unrobust to external disturbances and model uncertainty.

A first work taking this direction is [13], which proposes a variation of the integral IDA-PBC technique for soft manipulators. This strategy still relies on model-based cancellations and, as such, it is potentially unrobust to model uncertainties. Remarkably, [14], [15], [16] investigated experimentally the use of PID regulators for controlling the shape of soft robots. However, these references do not provide stability proof and assume full actuation. We follow an alternative path with our recent works [17], [18], [19]. There, we proposed PD+ control laws for two classes of soft robots: elastically dominated and elastically decoupled. The goal is to have simple – and thus robust – controllers that are provably stable in the general setting and parsimoniously use the information on the robot dynamics. In this letter, we move a further step toward developing robust and simple shape regulators for soft robots under non-rough discretizations by adding a saturated integral (satI) action to the regulators of [17] and [18]. Fig. 1 shows a block scheme of the proposed control architecture. Including an integral term requires extreme care because the dynamic couplings with the soft robot dynamics may lead to instability. In addition to stability, we prove that (i) the steady state elastic force is learned through the integral term. As a result, the stiffness completely disappears from the control laws, avoiding the need to estimate its value accurately. Furthermore, in analogy with the internal model principle, (ii) the closed-loop system rejects matched constant disturbances.

Manuscript received 14 July 2022; accepted 24 October 2022. Date of publication 10 November 2022; date of current version 28 November 2022. This letter was recommended for publication by Associate Editor X. Li and Editor C. Gosselin upon evaluation of the reviewers' comments. *(Corresponding author: Pietro Pustina.)*

Pietro Pustina and Alessandro De Luca are with the Department of Computer, Control and Management Engineering, Sapienza University of Rome, 00185 Rome, Italy (e-mail: pietro.pustina@uniroma1.it; deluca@diag.uniroma1.it).

Pablo Borja is with the School of Engineering, Computing and Mathematics, University of Plymouth, PL4 8AA Plymouth, U.K. (e-mail: luisp-borja@gmail.com).

Cosimo Della Santina is with the Department of Cognitive Robotics, Delft University of Technology, 2628 CN Delft, The Netherlands, and also with the Institute of Robotics and Mechatronics, German Aerospace Center (DLR), 82234 Oberpfaffenhofen, Germany (e-mail: cosimodellasantina@gmail.com).

This letter has supplementary downloadable material available at https://doi.org/10.1109/LRA.2022.3221304, provided by the authors.

Digital Object Identifier 10.1109/LRA.2022.3221304

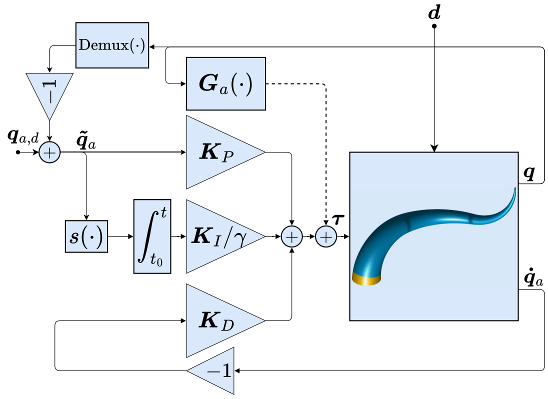

Fig. 1. Block scheme representation of the proposed control architecture. For elastically dominated soft robots, the control action is the sum of three terms: (i) a proportional, (ii) a derivative, and (iii) a saturated integral action driven by the tracking error. The regulator for elastically decoupled soft robots requires an additional term, illustrated with a black dashed line, that cancels the gravitational forces on the actuated variables.

II. Preliminaries

A. Notation

Vectors and matrices are denoted with bold lower- and uppercase letters, respectively, whereas scalars with lowercase normal ones. The symbol $\boldsymbol{I}_n$ represents the $n \times n$ identity matrix. Zero vectors and matrices of proper dimension are denoted as $\mathbf{0}$ and $\boldsymbol{O}$, respectively. For a vector $\boldsymbol{x} \in \mathbb{R}^h$, its p-norm is denoted as $\|\boldsymbol{x}\|_p, p \geq 2$ and for $p = 2$ simply $\|\boldsymbol{x}\|$. Similarly, if $\boldsymbol{A} \in \mathbb{R}^{h \times l}$, $\|\boldsymbol{A}\|$ is the matrix norm induced by the Euclidean norm of vectors. Given a symmetric matrix $\boldsymbol{A}$, i.e., $\boldsymbol{A} = \boldsymbol{A}^T$, its smallest and largest eigenvalues are $\lambda_{\min}(\boldsymbol{A})$ and $\lambda_{\max}(\boldsymbol{A})$. If $\lambda_{\min}(\boldsymbol{A}) > 0$ (or ≥ 0), then $\boldsymbol{A}$ is said to be positive definite (or semidefinite), and it is denoted as $\boldsymbol{A} > 0$ (or $\boldsymbol{A} \geq 0$). To simplify the notation, arguments of the functions are omitted when clear from the context. Furthermore, given a continuously differentiable function $f(\boldsymbol{x}) : \mathbb{R}^h \to \mathbb{R}$, $\boldsymbol{\nabla}_{\boldsymbol{x}}(f) \in \mathbb{R}^h$ and $\boldsymbol{\nabla}^2_{\boldsymbol{x}}(f) \in \mathbb{R}^{h \times h}$ denote, respectively, the gradient and Hessian of f. For $\boldsymbol{g}(\boldsymbol{x}) : \mathbb{R}^h \to \mathbb{R}^l$, its Jacobian is $\boldsymbol{J}_{\boldsymbol{x}}(\boldsymbol{g}) \in \mathbb{R}^{l \times h}$.

B. Dynamic Model

Consider a continuum soft robot described by

$$\begin{aligned} &\boldsymbol{M}_{\boldsymbol{\theta}}(\boldsymbol{\theta})\ddot{\boldsymbol{\theta}} + \boldsymbol{C}_{\boldsymbol{\theta}}(\boldsymbol{\theta}, \dot{\boldsymbol{\theta}})\dot{\boldsymbol{\theta}} + \boldsymbol{G}_{\boldsymbol{\theta}}(\boldsymbol{\theta}) \\ &\quad + \boldsymbol{K}_{\boldsymbol{\theta}}\boldsymbol{\theta} + \boldsymbol{D}_{\boldsymbol{\theta}}(\boldsymbol{\theta})\dot{\boldsymbol{\theta}} = \boldsymbol{A}(\boldsymbol{\tau} + \boldsymbol{d}), \end{aligned} \tag{1}$$

where $\boldsymbol{\theta} \in \mathbb{R}^n$ denotes the configuration vector, $\boldsymbol{M}_{\boldsymbol{\theta}}(\boldsymbol{\theta}) > 0$ is the mass matrix, $\boldsymbol{C}_{\boldsymbol{\theta}}(\boldsymbol{\theta}, \dot{\boldsymbol{\theta}})\dot{\boldsymbol{\theta}}$ collects Coriolis and centrifugal effects, and $\boldsymbol{G}_{\boldsymbol{\theta}}(\boldsymbol{\theta}) = \boldsymbol{\nabla}_{\boldsymbol{\theta}}(U_g(\boldsymbol{\theta}))$ contains the forces due to gravity, being $U_g(\boldsymbol{\theta})$ the gravitational potential energy. Elastic and dissipation forces are modeled, respectively, through $\boldsymbol{K}_{\boldsymbol{\theta}}\boldsymbol{\theta}$ and $\boldsymbol{D}_{\boldsymbol{\theta}}(\boldsymbol{\theta})\dot{\boldsymbol{\theta}}$, with $\boldsymbol{K}_{\boldsymbol{\theta}} > 0$ and $\boldsymbol{D}_{\boldsymbol{\theta}}(\boldsymbol{\theta}) > 0$. Finally, $\boldsymbol{\tau} \in \mathbb{R}^m$ groups the generalized input forces, projected into the configuration space through the constant actuation matrix $\boldsymbol{A} \in \mathbb{R}^{n \times m}$, and $\boldsymbol{d} \in \mathbb{R}^m$ is a constant disturbance, i.e., $\dot{\boldsymbol{d}} = \mathbf{0}$. In [18] it is shown that (1) includes a reasonably large class of soft robots. Indeed, if the columns of $\boldsymbol{A}$ are linearly independent, it is always possible to define a linear change of coordinates $\boldsymbol{q} = \boldsymbol{T}\boldsymbol{\theta}$ such that the dynamics becomes

$$\begin{aligned} &\overbrace{\begin{pmatrix} \boldsymbol{M}_{aa} & \boldsymbol{M}_{au} \\ \boldsymbol{M}_{ua} & \boldsymbol{M}_{uu} \end{pmatrix}}^{\boldsymbol{M}(\boldsymbol{q})} \begin{pmatrix} \ddot{\boldsymbol{q}}_a \\ \ddot{\boldsymbol{q}}_u \end{pmatrix} + \overbrace{\begin{pmatrix} \boldsymbol{C}_{aa} & \boldsymbol{C}_{au} \\ \boldsymbol{C}_{ua} & \boldsymbol{C}_{uu} \end{pmatrix}}^{\boldsymbol{C}(\boldsymbol{q},\dot{\boldsymbol{q}})} \begin{pmatrix} \dot{\boldsymbol{q}}_a \\ \dot{\boldsymbol{q}}_u \end{pmatrix} + \overbrace{\begin{pmatrix} \boldsymbol{G}_a \\ \boldsymbol{G}_u \end{pmatrix}}^{\boldsymbol{G}(\boldsymbol{q})} \\ &+ \underbrace{\begin{pmatrix} \boldsymbol{K}_{aa} & \boldsymbol{K}_{au} \\ \boldsymbol{K}_{ua} & \boldsymbol{K}_{uu} \end{pmatrix}}_{\boldsymbol{K}} \begin{pmatrix} \boldsymbol{q}_a \\ \boldsymbol{q}_u \end{pmatrix} + \underbrace{\begin{pmatrix} \boldsymbol{D}_{aa} & \boldsymbol{D}_{au} \\ \boldsymbol{D}_{ua} & \boldsymbol{D}_{uu} \end{pmatrix}}_{\boldsymbol{D}(\boldsymbol{q})} \begin{pmatrix} \dot{\boldsymbol{q}}_a \\ \dot{\boldsymbol{q}}_u \end{pmatrix} = \begin{pmatrix} \boldsymbol{\tau} + \boldsymbol{d} \\ \mathbf{0} \end{pmatrix}, \end{aligned} \tag{2}$$

where the configuration vector $\boldsymbol{q}$ has been divided into actuated and unactuated variables, denoted from now on $\boldsymbol{q}_a \in \mathbb{R}^m$ and $\boldsymbol{q}_u \in \mathbb{R}^{n-m}$, respectively, and the dynamic terms have been partitioned accordingly.

C. Properties

Without loss of generality, the dynamic model (2) satisfies a set of properties previously reported for robots with revolute joints [20], which we list below for the sake of readability.

Property 1: There exist constants $k_M, k_m > 0$ such that, for all $\boldsymbol{q}, \boldsymbol{x} \in \mathbb{R}^n$,

$$k_m\|\boldsymbol{x}\|^2 \leq \boldsymbol{x}^T\boldsymbol{M}(\boldsymbol{q})\boldsymbol{x} \leq k_M\|\boldsymbol{x}\|^2.$$

Property 2: There exists a constant $k_C > 0$ such that, for all $\boldsymbol{q}, \dot{\boldsymbol{q}} \in \mathbb{R}^n$,

$$\|\boldsymbol{C}(\boldsymbol{q}, \dot{\boldsymbol{q}})\dot{\boldsymbol{q}}\| \leq k_C\|\dot{\boldsymbol{q}}\|^2.$$

In addition, $\dot{\boldsymbol{M}}(\boldsymbol{q}) - 2\boldsymbol{C}(\boldsymbol{q}, \dot{\boldsymbol{q}})$ is skew symmetric or, equivalently, $\dot{\boldsymbol{M}}(\boldsymbol{q}) = \boldsymbol{C}(\boldsymbol{q}, \dot{\boldsymbol{q}}) + \boldsymbol{C}^T(\boldsymbol{q}, \dot{\boldsymbol{q}})$.

Property 3: There exist constants $k_{U_g}, k_G, k_{\partial G} > 0$ such that, for all $\boldsymbol{q} \in \mathbb{R}^n$,

$$\|U_g(\boldsymbol{q})\| \leq k_{U_g},\ \ \|\boldsymbol{G}(\boldsymbol{q})\| \leq k_G,\ \ \|\boldsymbol{J}_{\boldsymbol{q}}(\boldsymbol{G}(\boldsymbol{q}))\| \leq k_{\partial G}.$$

D. A Class of Saturated Functions

In Sections III and IV, control laws for shape regulation of two classes of underactuated soft robots are presented. These extend the controllers of [17], [18] by adding an integral action driven by the following class of saturated functions.

Definition 1: Let $\mathcal{S}(\beta, \alpha_1, \alpha_2, \alpha_3)$ be the set of $\mathcal{C}^1$ monotonically increasing functions $\boldsymbol{s}(\boldsymbol{x}) = (s(x_1)\ s(x_2) \cdots s(x_h))^T : \mathbb{R}^h \to \mathbb{R}^h$ such that, for all $y \in \mathbb{R}$,

i) $s(y) = \sigma(y)y$ holds for a function $\sigma : \mathbb{R} \to \mathbb{R}$ defined everywhere,

ii) $|s(y)| \geq \begin{cases} \alpha_1|y|; & |y| \leq \beta \\ \alpha_1\beta\,; & |y| > \beta \end{cases}$,

iii) $|s(y)| \leq \begin{cases} |y|; & |y| \leq \beta \\ \beta\,; & |y| > \beta \end{cases}$,

iv) $\alpha_2 \geq \dfrac{ds(y)}{dy} \geq 0$,

v) $\left|1 - \dfrac{ds(y)}{dy}\right| \leq \alpha_3|s(y)|$.

For example, $\boldsymbol{s}_t(\boldsymbol{x}) = (s_t(x_1) \cdots s_t(x_h))$, $s_t(y) = \tanh(y)$, belongs to $\mathcal{S}(1, \tanh(1), 1, 1)$. Another example is $\boldsymbol{s}_p(\boldsymbol{x}) = (s_p(x_1) \cdots s_p(x_h))$, $s_p(y) = \frac{y}{(1+|y|^p)^{\frac{1}{p}}}$ and $p \in \mathbb{Z}_+$, which belongs to $\mathcal{S}(1, 2^{-\frac{1}{p}}, 1, 1)$.

The above class of functions satisfies a series of useful properties. In particular, for all $\boldsymbol{x} \in \mathbb{R}^h$ and $\boldsymbol{Q} \in \mathbb{R}^{h \times h}$ symmetric, we have the following.

Property 4: ([21]) Given $k_1 = \alpha_1$, $k_2 = \alpha_1\beta$, and $k_3 = \sqrt{h}\beta$,
the following inequalities hold

$$\|\boldsymbol{s}(\boldsymbol{x})\| \geq \begin{cases} k_1\|\boldsymbol{x}\|; & \|\boldsymbol{x}\| \leq \beta \\ k_2 \quad ; & \|\boldsymbol{x}\| > \beta, \end{cases}$$

and

$$\|\boldsymbol{s}(\boldsymbol{x})\| \leq \begin{cases} \|\boldsymbol{x}\|; & \|\boldsymbol{x}\| \leq \beta \\ k_3\,; & \|\boldsymbol{x}\| > \beta. \end{cases}$$

Property 5: ([21]) $\boldsymbol{s}^T(\boldsymbol{x})\boldsymbol{x} \geq \begin{cases} k_1\|\boldsymbol{x}\|^2; & \|\boldsymbol{x}\| \leq \beta \\ k_2\|\boldsymbol{x}\| \;; & \|\boldsymbol{x}\| > \beta. \end{cases}$

Property 6: $\lambda_{\max}(\boldsymbol{Q})\boldsymbol{s}^T(\boldsymbol{x})\boldsymbol{x} \geq \boldsymbol{s}^T(\boldsymbol{x})\boldsymbol{Q}\boldsymbol{x} \geq \lambda_{\min}(\boldsymbol{Q})$ $\boldsymbol{s}^T(\boldsymbol{x})\boldsymbol{x}$.

Proof: We prove only the right-hand side of the above inequality because similar arguments can also be used for the left-hand side. From (i) it follows that $\boldsymbol{s}(\boldsymbol{x}) = \boldsymbol{\Sigma}(\boldsymbol{x})\boldsymbol{x}$, where $\boldsymbol{\Sigma}(\boldsymbol{x}) = \text{diag}\{\sigma(x_1)\cdots\sigma(x_h)\}$, which yields $\boldsymbol{s}^T(\boldsymbol{x})\boldsymbol{Q}\boldsymbol{x} = \boldsymbol{x}^T\boldsymbol{\Sigma}(\boldsymbol{x})\boldsymbol{Q}\boldsymbol{x}$. Furthermore, the monotonicity of $s(y)$ and (i) imply that $\sigma(y) > 0$ and, consequently, $\boldsymbol{\Sigma}(\boldsymbol{x}) > 0$. Thus, $\boldsymbol{s}^T(\boldsymbol{x})\boldsymbol{Q}\boldsymbol{x} \geq \lambda_{\min}(\boldsymbol{Q})\boldsymbol{s}^T(\boldsymbol{x})\boldsymbol{x}$ is equivalent to

$$\boldsymbol{x}^T\boldsymbol{\Sigma}(\boldsymbol{x})\left(\boldsymbol{Q} - \lambda_{\min}(\boldsymbol{Q})\boldsymbol{I}_h\right)\boldsymbol{x} \geq 0.$$

Being $\boldsymbol{\Sigma}(\boldsymbol{x}) > 0$ and $\boldsymbol{Q} - \lambda_{\min}(\boldsymbol{Q})\boldsymbol{I}_h \geq 0$ and symmetric, $\boldsymbol{\Sigma}(\boldsymbol{x})(\boldsymbol{Q} - \lambda_{\min}(\boldsymbol{x})\boldsymbol{I}_h) \geq 0$ [22]. □

Property 7: Given $k_4 = \alpha_2$ and $k_5 = \alpha_3$, the following inequalities hold

$$\|\boldsymbol{J}_{\boldsymbol{x}}(\boldsymbol{s}(\boldsymbol{x}))\| \leq k_4, \quad \|\boldsymbol{I}_h - \boldsymbol{J}_{\boldsymbol{x}}(\boldsymbol{s}(\boldsymbol{x}))\| \leq k_5\|\boldsymbol{s}(\boldsymbol{x})\|.$$

Proof: The first inequality follows observing that $\boldsymbol{J}_{\boldsymbol{x}}(\boldsymbol{s}(\boldsymbol{x}))$ is a diagonal matrix. The second is an immediate consequence of $|s(x_i)| \leq \|\boldsymbol{s}(\boldsymbol{x})\|$. □

The set $\mathcal{S}$ takes inspiration from previous works on PID control with saturated integral action of rigid robots [21], [23]. However, the actual context does not allow using the class of saturation functions proposed in those references because Property 6, which enables exploiting the elasticity in the control laws and stability proofs, is not generally valid.

III. P-SatI-D+ Control For Elastically Decoupled Soft Robots

This section presents a PID controller with saturated integral action and gravity cancellation for shape regulation of elastically decoupled soft robots. To this end, we first introduce the following definition.

Definition 2: A soft robot is said to be *elastically decoupled* if there is no elastic coupling between the actuated and unactuated variables, i.e.,

$$\boldsymbol{K} = \begin{pmatrix} \boldsymbol{K}_{aa} & \boldsymbol{O} \\ \boldsymbol{O} & \boldsymbol{K}_{uu} \end{pmatrix}. \tag{4}$$

Note that no special condition on $\boldsymbol{K}_{uu}$ is needed, except that $\boldsymbol{K}_{uu} > 0$. To extend the PD+ regulator presented in [17], we add a saturated integral action driven by the tracking error of the actuated variables. In particular, we consider the collocated control law

$$\boldsymbol{\tau} = \boldsymbol{K}_P\tilde{\boldsymbol{q}}_a - \boldsymbol{K}_D\dot{\boldsymbol{q}}_a + \frac{\boldsymbol{K}_I}{\gamma}\int_0^t \boldsymbol{s}(\tilde{\boldsymbol{q}}_a(\rho))d\rho + \boldsymbol{G}_a(\boldsymbol{q}), \tag{5}$$

where $\tilde{\boldsymbol{q}}_a := \boldsymbol{q}_{a,d} - \boldsymbol{q}_a$ is the tracking error with $\boldsymbol{q}_{a,d}$ the desired set point, $\boldsymbol{K}_P > 0$, $\boldsymbol{K}_D \geq 0$, $\boldsymbol{K}_I > 0$, $\gamma > 0$ are control gains, and $\boldsymbol{s}(\tilde{\boldsymbol{q}}_a) \in \mathcal{S}(\beta, \alpha_1, \alpha_2, \alpha_3)$.

The following theorem shows that the control law (5), which we call *P-satI-D+*, guarantees bounded closed-loop trajectories and asymptotic convergence of $\tilde{\boldsymbol{q}}_a$ to $\boldsymbol{0}$, provided that $\boldsymbol{K}_P$ and γ are appropriately tuned.

Theorem 1: For an elastically decoupled soft robot there exist finite constants $\alpha_P > 0$ and $\tilde{\gamma} > 0$ such that, for all $\boldsymbol{K}_P > \alpha_P\boldsymbol{I}_m$ and $\gamma > \tilde{\gamma}$, the trajectories of the closed-loop system (2)–(5) are bounded and converge asymptotically to the equilibrium $(\boldsymbol{q}_a\ \boldsymbol{q}_u\ \dot{\boldsymbol{q}}_a\ \dot{\boldsymbol{q}}_u) = (\boldsymbol{q}_{a,d}\ \boldsymbol{q}_{u,d}\ \boldsymbol{0}\ \boldsymbol{0})$, where $\boldsymbol{q}_{u,d}$ is a solution to

$$\boldsymbol{K}_{uu}\boldsymbol{q}_u + \boldsymbol{G}_u(\boldsymbol{q}_{a,d}, \boldsymbol{q}_u) = \boldsymbol{0}. \tag{6}$$

Proof: Defining the additional state variables

$$\boldsymbol{z}(t) := \int_0^t \boldsymbol{s}(\tilde{\boldsymbol{q}}_a(\rho))d\rho - \gamma\boldsymbol{K}_I^{-1}\left(\boldsymbol{K}_{aa}\boldsymbol{q}_{a,d} - \boldsymbol{d}\right),$$

the P-satI-D+ can be rewritten as

$$\boldsymbol{\tau} = \boldsymbol{K}_P\tilde{\boldsymbol{q}}_a - \boldsymbol{K}_D\dot{\boldsymbol{q}}_a + \frac{\boldsymbol{K}_I}{\gamma}\boldsymbol{z}(t) + \boldsymbol{K}_{aa}\boldsymbol{q}_{a,d} - \boldsymbol{d} + \boldsymbol{G}_a(\boldsymbol{q}),$$

which leads to the closed-loop (3), shown at the bottom of this page. Note also that $\boldsymbol{z}$ has the same dynamics of the integral. Consider the Lyapunov-like function

$$\begin{aligned} V(\tilde{\boldsymbol{q}}_a, \boldsymbol{q}_u, \dot{\boldsymbol{q}}, \boldsymbol{z}) = \gamma\Bigg(&\frac{1}{2}\dot{\boldsymbol{q}}^T\boldsymbol{M}\dot{\boldsymbol{q}} + U_g + \frac{1}{2}\tilde{\boldsymbol{q}}_a^T(\boldsymbol{K}_P + \boldsymbol{K}_{aa})\tilde{\boldsymbol{q}}_a \\ &+ \frac{1}{2}\boldsymbol{q}_u^T\boldsymbol{K}_{uu}\boldsymbol{q}_u + \boldsymbol{s}^T(\tilde{\boldsymbol{q}}_a)\boldsymbol{G}_a + \tilde{\boldsymbol{q}}_a^T\frac{\boldsymbol{K}_I}{\gamma}\boldsymbol{z}\Bigg) \\ &+ \frac{1}{2}\boldsymbol{z}^T\frac{\boldsymbol{K}_I}{\gamma}\boldsymbol{z} - \boldsymbol{s}^T(\tilde{\boldsymbol{q}}_a)\left(\boldsymbol{M}_{aa}\dot{\boldsymbol{q}}_a + \boldsymbol{M}_{au}\dot{\boldsymbol{q}}_u\right), \end{aligned}$$

which is radially unbounded since

$$\begin{aligned} V \geq\ &\frac{\gamma}{2}k_m\|\dot{\boldsymbol{q}}\|^2 - \gamma k_{U_g} + \frac{\gamma}{2}\lambda_{\min}(\boldsymbol{K}_{aa} + \boldsymbol{K}_P)\|\tilde{\boldsymbol{q}}_a\|^2 \\ &+ \frac{\gamma}{2}\lambda_{\min}(\boldsymbol{K}_{uu})\|\boldsymbol{q}_u\|^2 - \gamma k_3 k_G - \lambda_{\max}(\boldsymbol{K}_I)\|\tilde{\boldsymbol{q}}_a\|\|\boldsymbol{z}\| \\ &- k_3 k_M\|\dot{\boldsymbol{q}}\| + \frac{\lambda_{\min}(\boldsymbol{K}_I)}{2\gamma}\|\boldsymbol{z}\|^2, \end{aligned}$$

and the right-hand-side of the above inequality diverges to $+\infty$ as $\|(\tilde{\boldsymbol{q}}_a\ \boldsymbol{q}_u\ \dot{\boldsymbol{q}}\ \boldsymbol{z})\|$ tends to ∞.

$$\boldsymbol{M}(\boldsymbol{q})\ddot{\boldsymbol{q}} + \boldsymbol{C}(\boldsymbol{q}, \dot{\boldsymbol{q}})\dot{\boldsymbol{q}} + \boldsymbol{G}(\boldsymbol{q}) + \boldsymbol{K}\boldsymbol{q} + \boldsymbol{D}\dot{\boldsymbol{q}} = \begin{pmatrix} \boldsymbol{K}_P\tilde{\boldsymbol{q}}_a - \boldsymbol{K}_D\dot{\boldsymbol{q}}_a + \boldsymbol{K}_I\boldsymbol{z} + \boldsymbol{G}_a(\boldsymbol{q}) + \boldsymbol{K}_{aa}\boldsymbol{q}_{a,d} \\ \boldsymbol{0} \end{pmatrix}, \qquad \dot{\boldsymbol{z}} = \boldsymbol{s}(\tilde{\boldsymbol{q}}_a). \tag{3}$$

Taking the time derivative of V along the trajectories of the closed-loop system yields

$$\begin{aligned}\dot{V} = \gamma \Big(&\frac{1}{2}\dot{\boldsymbol{q}}^T \dot{\boldsymbol{M}}\dot{\boldsymbol{q}} + \dot{\boldsymbol{q}}^T \boldsymbol{M}\ddot{\boldsymbol{q}} + \dot{\boldsymbol{q}}^T \boldsymbol{G} - \dot{\boldsymbol{q}}_a^T (\boldsymbol{K}_P + \boldsymbol{K}_{aa})\tilde{\boldsymbol{q}}_a \\ &+ \dot{\boldsymbol{q}}_u^T \boldsymbol{K}_{uu}\boldsymbol{q}_u - \dot{\boldsymbol{q}}_a^T \boldsymbol{J}_{\tilde{\boldsymbol{q}}_a}^T(\boldsymbol{s})\boldsymbol{G}_a + \boldsymbol{s}^T(\tilde{\boldsymbol{q}}_a)\boldsymbol{J}_{\boldsymbol{q}}(\boldsymbol{G}_a)\dot{\boldsymbol{q}} \\ &- \dot{\boldsymbol{q}}_a^T \frac{\boldsymbol{K}_I}{\gamma}\boldsymbol{z} + \tilde{\boldsymbol{q}}_a^T \frac{\boldsymbol{K}_I}{\gamma}\boldsymbol{s}(\tilde{\boldsymbol{q}}_a)\Big) + \boldsymbol{s}(\tilde{\boldsymbol{q}}_a)^T \frac{\boldsymbol{K}_I}{\gamma}\boldsymbol{z} \\ &- \boldsymbol{s}^T(\tilde{\boldsymbol{q}}_a)\left(\dot{\boldsymbol{M}}_{aa}\dot{\boldsymbol{q}}_a + \dot{\boldsymbol{M}}_{au}\dot{\boldsymbol{q}}_u + \boldsymbol{M}_{aa}\ddot{\boldsymbol{q}}_a + \boldsymbol{M}_{au}\ddot{\boldsymbol{q}}_u\right) \\ &+ \dot{\boldsymbol{q}}_a^T \boldsymbol{J}_{\tilde{\boldsymbol{q}}_a}^T(\boldsymbol{s})(\boldsymbol{M}_{aa}\dot{\boldsymbol{q}}_a + \boldsymbol{M}_{au}\dot{\boldsymbol{q}}_u).\end{aligned}$$

Replacing (3) in the above equation one obtains

$$\begin{aligned}\dot{V} = \gamma &\left(-\dot{\boldsymbol{q}}^T \tilde{\boldsymbol{D}}\dot{\boldsymbol{q}} + \dot{\boldsymbol{q}}_a^T \left(\boldsymbol{I}_m - \boldsymbol{J}_{\tilde{\boldsymbol{q}}_a}^T(\boldsymbol{s})\right)\boldsymbol{G}_a + \boldsymbol{s}^T(\tilde{\boldsymbol{q}}_a)\boldsymbol{J}_{\boldsymbol{q}}(\boldsymbol{G}_a)\dot{\boldsymbol{q}}\right) \\ &+ \dot{\boldsymbol{q}}_a^T \boldsymbol{J}_{\tilde{\boldsymbol{q}}_a}^T(\boldsymbol{s})\left(\boldsymbol{M}_{aa}\dot{\boldsymbol{q}}_a + \boldsymbol{M}_{au}\dot{\boldsymbol{q}}_u\right) + \boldsymbol{s}^T(\tilde{\boldsymbol{q}}_a)\tilde{\boldsymbol{D}}_a\dot{\boldsymbol{q}} \\ &+ \boldsymbol{s}^T(\tilde{\boldsymbol{q}}_a)\left(\boldsymbol{C}_{aa}^T\dot{\boldsymbol{q}}_a + \boldsymbol{C}_{ua}^T\dot{\boldsymbol{q}}_u\right) - \boldsymbol{s}^T(\tilde{\boldsymbol{q}}_a)\tilde{\boldsymbol{K}}_{aa}\tilde{\boldsymbol{q}}_a,\end{aligned}$$

where we defined

$$\tilde{\boldsymbol{D}} = \begin{pmatrix}\tilde{\boldsymbol{D}}_a \\ \tilde{\boldsymbol{D}}_u\end{pmatrix} := \boldsymbol{D} + \begin{pmatrix}\boldsymbol{K}_D & \boldsymbol{O} \\ \boldsymbol{O} & \boldsymbol{O}\end{pmatrix},$$

$$\tilde{\boldsymbol{K}}_{aa} := \boldsymbol{K}_{aa} + \boldsymbol{K}_P - \boldsymbol{K}_I.$$

Note that

$$\begin{aligned}\gamma\dot{\boldsymbol{q}}_a^T\left(\boldsymbol{I}_m - \boldsymbol{J}_{\tilde{\boldsymbol{q}}_a}^T(\boldsymbol{s})\right)\boldsymbol{G}_a &\le \gamma k_G k_5 \|\boldsymbol{s}(\tilde{\boldsymbol{q}}_a)\|\|\dot{\boldsymbol{q}}\|, \\ \gamma\boldsymbol{s}^T(\tilde{\boldsymbol{q}}_a)\boldsymbol{J}_{\boldsymbol{q}}(\boldsymbol{G}_a)\dot{\boldsymbol{q}} &\le \gamma k_{\partial G}\|\boldsymbol{s}(\tilde{\boldsymbol{q}}_a)\|\|\dot{\boldsymbol{q}}\|, \\ \boldsymbol{s}^T(\tilde{\boldsymbol{q}}_a)\tilde{\boldsymbol{D}}_a\dot{\boldsymbol{q}} &\le \lambda_{\max}(\tilde{\boldsymbol{D}})\|\boldsymbol{s}(\tilde{\boldsymbol{q}}_a)\|\|\dot{\boldsymbol{q}}\|, \\ \dot{\boldsymbol{q}}_a^T\boldsymbol{J}_{\tilde{\boldsymbol{q}}_a}^T(\boldsymbol{s})\left(\boldsymbol{M}_{aa}\dot{\boldsymbol{q}}_a + \boldsymbol{M}_{au}\dot{\boldsymbol{q}}_u\right) &\le k_4 k_M\|\dot{\boldsymbol{q}}\|^2, \\ -\boldsymbol{s}^T(\tilde{\boldsymbol{q}}_a)\left(\boldsymbol{C}_{aa}^T\dot{\boldsymbol{q}}_a + \boldsymbol{C}_{ua}^T\dot{\boldsymbol{q}}_u\right) &\le k_3 k_C\|\dot{\boldsymbol{q}}\|^2.\end{aligned}$$

Hence, we get

$$\begin{aligned}\dot{V} \le &-\left(\gamma\lambda_{\min}(\tilde{\boldsymbol{D}}) - (k_4k_M + k_3k_C)\right)\|\dot{q}\|^2 \\ &+ \left(\gamma(k_Gk_5 + k_{\partial G}) + \lambda_{\max}(\tilde{\boldsymbol{D}})\right)\|\boldsymbol{s}(\tilde{\boldsymbol{q}}_a)\|\|\dot{q}\| \\ &- \lambda_{\min}(\tilde{\boldsymbol{K}}_{aa})\boldsymbol{s}^T(\tilde{\boldsymbol{q}}_a)\tilde{\boldsymbol{q}}_a. \quad (7)\end{aligned}$$

In view of Properties 4–6, for $\|\tilde{\boldsymbol{q}}_a\| \le \beta$, $\dot{V}$ is bounded by

$$\dot{V} \le -\begin{pmatrix}\|\dot{\boldsymbol{q}}\| \\ \|\tilde{\boldsymbol{q}}_a\|\end{pmatrix}^T \begin{pmatrix}Q_{11} & Q_{12} \\ Q_{12} & k_1Q_{22}\end{pmatrix}\begin{pmatrix}\|\boldsymbol{q}\| \\ \|\tilde{\boldsymbol{q}}_a\|\end{pmatrix},$$

with

$$\begin{aligned}Q_{11} &= \gamma\lambda_{\min}(\tilde{\boldsymbol{D}}) - (k_4k_M + k_3k_C), \\ Q_{12} &= -\frac{1}{2}\left(\gamma(k_Gk_5 + k_{\partial G}) + \lambda_{\max}(\tilde{\boldsymbol{D}})\right), \\ Q_{22} &= \lambda_{\min}(\tilde{\boldsymbol{K}}_{aa}).\end{aligned}$$

According to Sylvester's criterion, $\boldsymbol{Q}$ is positive definite if and only if

$$Q_{11} > 0, \quad \det\boldsymbol{Q} > 0.$$

Both conditions can be fulfilled by taking

$$\gamma > \tilde{\gamma} := \frac{k_4k_M + k_3k_C}{\lambda_{\min}(\tilde{\boldsymbol{D}})},$$

and

$$\begin{aligned}\lambda_{\min}(\boldsymbol{K}_P) > \alpha_{P,1} := &-\lambda_{\min}(\boldsymbol{K}_{aa}) + \lambda_{\max}(\boldsymbol{K}_I) \\ &+ \frac{\left(\gamma(k_Gk_5 + k_{\partial G}) + \lambda_{\max}(\tilde{\boldsymbol{D}})\right)^2}{4k_1\left(\gamma\lambda_{\min}(\tilde{\boldsymbol{D}}) - (k_4k_M + k_3k_C)\right)}.\end{aligned}$$

On the other hand, for $\|\tilde{\boldsymbol{q}}_a\| > \beta$, it is possible to write

$$\dot{V} < -Q_{11}\|\dot{\boldsymbol{q}}\|^2 + Q_{12}k_3\|\dot{\boldsymbol{q}}\| - k_2Q_{22}\beta,$$

which is a quadratic function in $\|\dot{\boldsymbol{q}}\|$ pointing downward. Consequently, $\dot{V} < 0$ if and only if its minimum value is negative, i.e.,

$$k_2Q_{22}\beta > k_3^2\frac{Q_{12}^2}{4Q_{11}} \;\equiv\; Q_{22} > \frac{k_3^2}{k_2\beta}\frac{Q_{12}^2}{4Q_{11}},$$

which is satisfied for

$$\begin{aligned}\lambda_{\min}(\boldsymbol{K}_P) > \alpha_{P,2} := &-\lambda_{\min}(\boldsymbol{K}_{aa}) + \lambda_{\max}(\boldsymbol{K}_I) \\ &+ \frac{k_3^2}{k_2\beta}\frac{\left(\gamma(k_Gk_5 + k_{\partial G}) + \lambda_{\max}(\tilde{\boldsymbol{D}})\right)^2}{4\left(\gamma\lambda_{\min}(\tilde{\boldsymbol{D}}) - (k_4k_M + k_3k_C)\right)}.\end{aligned}$$

Thus, if $\lambda_{\min}(\boldsymbol{K}_P) > \alpha_P := \max\{\alpha_{P,1}; \alpha_{P,2}\}$, then $\dot{V} \le 0$. The thesis follows applying the Global Invariant Set theorem [24], and noting that $\dot{V} = 0$ if and only if $\tilde{\boldsymbol{q}}_a = \boldsymbol{0}$ and $\dot{\boldsymbol{q}} = \boldsymbol{0}$. □

Remark 1: Without further assumptions other than (4), there might exists more than one equilibrium for the unactuated variables compatible with that reached by the actuated ones. Thus, even if $\boldsymbol{q}_a$ converges asymptotically to $\boldsymbol{q}_{a,d}$, the system does not have a globally asymptotically stable equilibrium in general.

IV. P-SatI-D Control For Elastically Dominated Soft Robots

In this section, we present our main result for elastically dominated soft robots. First, the following statement defines what an elastically dominated soft robot is.

Definition 3: A soft robot with stiffness matrix

$$\boldsymbol{K} = \begin{pmatrix}\boldsymbol{K}_{aa} & \boldsymbol{K}_{au} \\ \boldsymbol{K}_{ua} & \boldsymbol{K}_{uu}\end{pmatrix}, \quad (8)$$

is said to be *elastically dominated* if it satisfies

$$\lambda_{\min}(\boldsymbol{K}_{uu}) > k_{\partial G}. \quad (9)$$

The inequality (9) guarantees that the potential field is convex with respect to the unactuated variables, implying that (6) admits a unique solution $\boldsymbol{q}_{u,d}$ for all $\boldsymbol{q}_{a,d}$. As a consequence, $\boldsymbol{q}_d = (\boldsymbol{q}_{a,d}^T\ \boldsymbol{q}_{u,d}^T)^T$ can be rendered globally asymptotically stable (GAS) by using the *P-satI-D* control law

$$\boldsymbol{\tau} = \boldsymbol{K}_P\tilde{\boldsymbol{q}}_a - \boldsymbol{K}_D\dot{\boldsymbol{q}}_a + \frac{\boldsymbol{K}_I}{\gamma}\int_0^t \boldsymbol{s}_a(\tilde{\boldsymbol{q}}(\rho))d\rho, \quad (10)$$

where $\tilde{\boldsymbol{q}} = \boldsymbol{q}_d - \boldsymbol{q}$ is the tracking error, $\boldsymbol{K}_P > 0$, $\boldsymbol{K}_D \ge 0$, $\boldsymbol{K}_I > 0$, $\gamma > 0$ are control gains, and $\boldsymbol{s}_a(\tilde{\boldsymbol{q}}) = \boldsymbol{s}(\tilde{\boldsymbol{q}}_a)$ denotes the first m components of $\boldsymbol{s}(\tilde{\boldsymbol{q}}) \in \mathcal{S}(\beta, \alpha_1, \alpha_2, \alpha_3)$. In analogy with Theorem 1, the following result formalizes that, if $\boldsymbol{K}_P$ and γ are large enough, then (10) ensures that $\boldsymbol{q}_d$ is a GAS equilibrium for the closed-loop system.

Theorem 2: For an elastically dominated soft robot there exist finite constants $\alpha_P > 0$ and $\tilde{\gamma} > 0$ such that, for all $\boldsymbol{K}_P > \alpha_P\boldsymbol{I}_m$ and $\gamma > \tilde{\gamma}$, the trajectories of the closed-loop system (2)–(10) are bounded and converge asymptotically to the equilibrium $(\boldsymbol{q}_a\ \boldsymbol{q}_u\ \dot{\boldsymbol{q}}_a\ \dot{\boldsymbol{q}}_u) = (\boldsymbol{q}_{a,d}\ \boldsymbol{q}_{u,d}\ \mathbf{0}\ \mathbf{0})$ where $\boldsymbol{q}_{u,d}$ is the unique solution to

$$\boldsymbol{G}_u(\boldsymbol{q}_{a,d}, \boldsymbol{q}_u) + \boldsymbol{K}_{ua}\boldsymbol{q}_{a,d} + \boldsymbol{K}_{uu}\boldsymbol{q}_u = \mathbf{0}. \tag{11}$$

Proof: To prove that (11) admits a unique solution, consider the function $P_u(\boldsymbol{q}_u) : \mathbb{R}^{n-m} \to \mathbb{R}$ defined as

$$P_u(\boldsymbol{q}_u) = U_g(\boldsymbol{q}_{a,d}, \boldsymbol{q}_u) + \frac{1}{2}\begin{pmatrix}\boldsymbol{q}_{a,d}\\ \boldsymbol{q}_u\end{pmatrix}^T \boldsymbol{K}\begin{pmatrix}\boldsymbol{q}_{a,d}\\ \boldsymbol{q}_u\end{pmatrix},$$

where U_g is bounded and $\boldsymbol{K} > 0$. Thus, P_u has (at least) a local minimum. Noting that $\boldsymbol{\nabla}_{\boldsymbol{q}_u}(P_u) = \boldsymbol{G}_u(\boldsymbol{q}_{a,d}, \boldsymbol{q}_u) + \boldsymbol{K}_{ua}\boldsymbol{q}_{a,d} + \boldsymbol{K}_{uu}\boldsymbol{q}_u$, it follows that $\boldsymbol{q}_{u,d}$ is an extremum of P_u. Furthermore, (9) implies that the Hessian of P_u is positive definite. Thus, P_u is strictly convex with unique global minimum given by the unique solution of (11). Defining the additional state variables

$$\boldsymbol{z}(t) := \int_0^t \boldsymbol{s}_a(\tilde{\boldsymbol{q}}(\rho))d\rho - \gamma\boldsymbol{K}_I^{-1}(\boldsymbol{K}_{aa}\boldsymbol{q}_{a,d} + \boldsymbol{K}_{au}\boldsymbol{q}_{u,d} + \boldsymbol{G}_a(\boldsymbol{q}_d) - \boldsymbol{d}),$$

and exploiting the identity $\boldsymbol{G}_u(\boldsymbol{q}_d) + \boldsymbol{K}_{ua}\boldsymbol{q}_{a,d} + \boldsymbol{K}_{uu}\boldsymbol{q}_{u,d} = \mathbf{0}$, the closed-loop dynamics takes the form (12), shown at the bottom of this page, where

$$\boldsymbol{\tau} = \boldsymbol{K}_P\tilde{\boldsymbol{q}}_a - \boldsymbol{K}_D\dot{\boldsymbol{q}}_a + \frac{\boldsymbol{K}_I}{\gamma}\boldsymbol{z}(t) + \boldsymbol{K}_{aa}\boldsymbol{q}_{a,d} + \boldsymbol{K}_{au}\boldsymbol{q}_{u,d} + \boldsymbol{G}_a(\boldsymbol{q}_d) - \boldsymbol{d}$$

has been used. Consider the Lyapunov-like function

$$\begin{aligned} V(\tilde{\boldsymbol{q}}, \dot{\boldsymbol{q}}, \boldsymbol{z}) = \gamma\Bigg(&\frac{1}{2}\dot{\boldsymbol{q}}^T\boldsymbol{M}\dot{\boldsymbol{q}} + U_g(\boldsymbol{q}) + \frac{1}{2}\tilde{\boldsymbol{q}}^T\boldsymbol{K}\tilde{\boldsymbol{q}} + \tilde{\boldsymbol{q}}^T\boldsymbol{G}(\boldsymbol{q}_d)\\ &+\frac{1}{2}\tilde{\boldsymbol{q}}_a^T\boldsymbol{K}_P\tilde{\boldsymbol{q}}_a + \tilde{\boldsymbol{q}}_a^T\frac{\boldsymbol{K}_I}{\gamma}\boldsymbol{z}\Bigg) + \frac{1}{2}\boldsymbol{z}^T\frac{\boldsymbol{K}_I}{\gamma}\boldsymbol{z}\\ &- \boldsymbol{s}^T(\tilde{\boldsymbol{q}})\boldsymbol{M}\dot{\boldsymbol{q}}, \end{aligned}$$

which is radially unbounded since

$$\begin{aligned} V \geq\ &\frac{\gamma}{2}k_m\|\dot{\boldsymbol{q}}\|^2 - \gamma k_U + \frac{\gamma}{2}\lambda_{\min}(\boldsymbol{K})\|\tilde{\boldsymbol{q}}\|^2\\ &- \gamma k_G\|\tilde{\boldsymbol{q}}\| + \frac{\gamma}{2}\lambda_{\min}(\boldsymbol{K}_P)\|\tilde{\boldsymbol{q}}_a\|^2\\ &- \lambda_{\max}(\boldsymbol{K}_I)\|\tilde{\boldsymbol{q}}_a\|\|\boldsymbol{z}\| + \frac{\lambda_{\min}(\boldsymbol{K}_I)}{2\gamma}\|\boldsymbol{z}\|^2\\ &- k_3k_M\|\dot{\boldsymbol{q}}\|, \end{aligned}$$

and the right-hand-side of the above inequality grows unbounded as $\|(\tilde{\boldsymbol{q}}\ \dot{\boldsymbol{q}}\ \boldsymbol{z})\|$ tends to ∞.

Taking the time derivative of V yields

$$\begin{aligned} \dot{V} = \gamma\Bigg(&\frac{1}{2}\dot{\boldsymbol{q}}^T\dot{\boldsymbol{M}}\dot{\boldsymbol{q}} + \dot{\boldsymbol{q}}^T\boldsymbol{M}\ddot{\boldsymbol{q}} + \dot{\boldsymbol{q}}^T\boldsymbol{G} - \dot{\boldsymbol{q}}^T(\boldsymbol{K}\tilde{\boldsymbol{q}} + \boldsymbol{G}(\boldsymbol{q}_d))\\ &- \dot{\boldsymbol{q}}_a^T\boldsymbol{K}_P\tilde{\boldsymbol{q}}_a - \dot{\boldsymbol{q}}_a^T\frac{\boldsymbol{K}_I}{\gamma}\boldsymbol{z} + \tilde{\boldsymbol{q}}_a^T\frac{\boldsymbol{K}_I}{\gamma}\boldsymbol{s}_a(\tilde{\boldsymbol{q}})\Bigg)\\ &+ \boldsymbol{s}_a^T(\tilde{\boldsymbol{q}})\frac{\boldsymbol{K}_I}{\gamma}\boldsymbol{z} + \dot{\boldsymbol{q}}^T\frac{\partial\boldsymbol{s}}{\partial\tilde{\boldsymbol{q}}}\boldsymbol{M}\dot{\boldsymbol{q}} - \boldsymbol{s}^T(\tilde{\boldsymbol{q}})(\dot{\boldsymbol{M}}\dot{\boldsymbol{q}} + \boldsymbol{M}\ddot{\boldsymbol{q}}). \end{aligned}$$

After some computations, (12) leads to

$$\begin{aligned} \dot{V} =\ &-\gamma\dot{\boldsymbol{q}}^T\tilde{\boldsymbol{D}}\dot{\boldsymbol{q}} + \dot{\boldsymbol{q}}^T\boldsymbol{J}_{\tilde{\boldsymbol{q}}}^T(\boldsymbol{s})\boldsymbol{M}\dot{\boldsymbol{q}} - \boldsymbol{s}^T(\tilde{\boldsymbol{q}})\boldsymbol{C}^T\dot{\boldsymbol{q}} + \boldsymbol{s}^T(\tilde{\boldsymbol{q}})\tilde{\boldsymbol{D}}\dot{\boldsymbol{q}}\\ &+ \boldsymbol{s}^T(\tilde{\boldsymbol{q}})(\boldsymbol{G}(\boldsymbol{q}) - \boldsymbol{G}(\boldsymbol{q}_d))\\ &- \boldsymbol{s}^T(\tilde{\boldsymbol{q}})\begin{pmatrix}\boldsymbol{K}_{aa} + \boldsymbol{K}_P - \boldsymbol{K}_I & \boldsymbol{K}_{au}\\ \boldsymbol{K}_{ua} & \boldsymbol{K}_{uu}\end{pmatrix}\tilde{\boldsymbol{q}}. \end{aligned}$$

Moreover, the following inequalities hold

$$\begin{aligned} \dot{\boldsymbol{q}}^T\boldsymbol{J}_{\tilde{\boldsymbol{q}}}^T(\boldsymbol{s})\boldsymbol{M}\dot{\boldsymbol{q}} &\leq k_4k_M\|\dot{\boldsymbol{q}}\|^2,\\ -\boldsymbol{s}^T(\tilde{\boldsymbol{q}})\boldsymbol{C}^T\dot{\boldsymbol{q}} &\leq k_3k_C\|\dot{\boldsymbol{q}}\|^2,\\ \boldsymbol{s}^T(\tilde{\boldsymbol{q}})\tilde{\boldsymbol{D}}\dot{\boldsymbol{q}} &\leq \lambda_{\max}(\tilde{\boldsymbol{D}})\|\boldsymbol{s}(\tilde{\boldsymbol{q}})\|\|\dot{\boldsymbol{q}}\|. \end{aligned}$$

Similarly, by the Mean Value theorem for vector-valued functions [25], it is possible to write

$$\boldsymbol{G}(\boldsymbol{q}) - \boldsymbol{G}(\boldsymbol{q}_d) = -\left(\int_0^1 \boldsymbol{J}_{\boldsymbol{x}}(\boldsymbol{G}(\boldsymbol{x}))_{\boldsymbol{x}=\boldsymbol{q}-s\tilde{\boldsymbol{q}}}ds\right)\tilde{\boldsymbol{q}}.$$

Recalling that $\boldsymbol{J}_{\boldsymbol{x}}(\boldsymbol{G}(\boldsymbol{x}))$ is symmetric, and invoking Properties 3 and 6, it follows

$$\boldsymbol{s}^T(\tilde{\boldsymbol{q}})(\boldsymbol{G}(\boldsymbol{q}) - \boldsymbol{G}(\boldsymbol{q}_d)) \leq k_{\partial G}\boldsymbol{s}^T(\tilde{\boldsymbol{q}})\tilde{\boldsymbol{q}}.$$

Thus,

$$\begin{aligned} \dot{V} \leq\ &-\left(\gamma\lambda_{\min}(\tilde{\boldsymbol{D}}) - (k_4k_M + k_3k_C)\right)\|\dot{\boldsymbol{q}}\|^2\\ &+ \lambda_{\max}(\tilde{\boldsymbol{D}})\|\boldsymbol{s}(\tilde{\boldsymbol{q}})\|\|\dot{\boldsymbol{q}}\| - \lambda_{\min}(\tilde{\boldsymbol{K}})\boldsymbol{s}^T(\tilde{\boldsymbol{q}})\tilde{\boldsymbol{q}}, \end{aligned}$$

where

$$\tilde{\boldsymbol{K}} := \begin{pmatrix}\boldsymbol{K}_{aa} + \boldsymbol{K}_P - \boldsymbol{K}_I - k_{\partial G}\boldsymbol{I}_m & \boldsymbol{K}_{au}\\ \boldsymbol{K}_{ua} & \boldsymbol{K}_{uu} - k_{\partial G}\boldsymbol{I}_{n-m}\end{pmatrix}.$$

Proceeding as in the proof of Theorem 1, we obtain, for $\|\tilde{\boldsymbol{q}}\| \leq \beta$,

$$\dot{V} \leq -\begin{pmatrix}\|\dot{\boldsymbol{q}}\|\\ \|\tilde{\boldsymbol{q}}\|\end{pmatrix}^T\begin{pmatrix}Q_{11} & Q_{12}\\ Q_{12} & k_1Q_{22}\end{pmatrix}\begin{pmatrix}\|\dot{\boldsymbol{q}}\|\\ \|\tilde{\boldsymbol{q}}\|\end{pmatrix},$$

with

$$\begin{aligned} Q_{11} &= \gamma\lambda_{\min}(\tilde{\boldsymbol{D}}) - (k_4k_M + k_3k_C),\\ Q_{12} &= -\frac{1}{2}\lambda_{\max}(\tilde{\boldsymbol{D}}),\ \ Q_{22} = \lambda_{\min}(\tilde{\boldsymbol{K}}). \end{aligned}$$

According to Sylvester's criterion, $\boldsymbol{Q} > 0$ if and only if

$$\lambda_{\min}(\tilde{\boldsymbol{K}}) > 0, \tag{13}$$

$$\det\boldsymbol{Q} > 0. \tag{14}$$

By Schur's criterion, (13) reduces to

$$\boldsymbol{K}_{uu} - k_{\partial G}\boldsymbol{I}_{n-m} > 0,$$

and

$$\boldsymbol{K}_P > \boldsymbol{K}_I + k_{\partial G}\boldsymbol{I}_m - \boldsymbol{K}_{aa} + \boldsymbol{K}_{au}(\boldsymbol{K}_{uu} - k_{\partial G}\boldsymbol{I}_{n-m})^{-1}\boldsymbol{K}_{ua}^T. \tag{15}$$

The first inequality holds from (9), while the latter can be enforced by choosing $\boldsymbol{K}_P$ large enough. Note that a sufficient

$$\boldsymbol{M}(\boldsymbol{q})\ddot{\boldsymbol{q}} + \boldsymbol{C}(\boldsymbol{q}, \dot{\boldsymbol{q}})\dot{\boldsymbol{q}} + \boldsymbol{G}(\boldsymbol{q}) + \boldsymbol{K}\boldsymbol{q} + \boldsymbol{D}\dot{\boldsymbol{q}} = \begin{pmatrix}\boldsymbol{K}_P\tilde{\boldsymbol{q}}_a - \boldsymbol{K}_D\dot{\boldsymbol{q}}_a + \frac{\boldsymbol{K}_I}{\gamma}\boldsymbol{z} + \boldsymbol{G}_a(\boldsymbol{q}_d) + \boldsymbol{K}_{aa}q_{a,d} + \boldsymbol{K}_{au}q_{u,d}\\ \boldsymbol{G}_u(\boldsymbol{q}_{a,d}, \boldsymbol{q}_{u,d}) + \boldsymbol{K}_{ua}\boldsymbol{q}_{a,d} + \boldsymbol{K}_{uu}\boldsymbol{q}_{u,d}\end{pmatrix}, \quad \dot{\boldsymbol{z}} = \boldsymbol{s}_a(\tilde{\boldsymbol{q}}). \tag{12}$$

condition to satisfy (15) is

$$\lambda_{\min}(\boldsymbol{K}_P) > \alpha_P := -\lambda_{\min}(\boldsymbol{K}_{aa}) + \lambda_{\max}(\boldsymbol{K}_I) + k_{\partial G} + \frac{\|\boldsymbol{K}_{au}\|^2}{\lambda_{\min}(K_{uu} - k_{\partial G}\boldsymbol{I}_{n-m})}.$$

Finally, (14) is guaranteed if

$$\gamma > \tilde{\gamma}_1 := \frac{1}{\lambda_{\min}(\tilde{\boldsymbol{D}})}\left(\frac{1}{k_1}\frac{\lambda^2_{\max}(\tilde{\boldsymbol{D}})}{4\lambda_{\min}(\tilde{\boldsymbol{K}})} + k_4 k_M + k_3 k_C\right).$$

Conversely, when $\|\tilde{\boldsymbol{q}}\| > \beta$, $\dot{V}$ is bounded by

$$\dot{V} < -Q_{11}\|\dot{\boldsymbol{q}}\|^2 + k_3 Q_{12}\|\dot{\boldsymbol{q}}\| - k_2\beta Q_{22},$$

which is negative if

$$Q_{11} > \frac{k_3^2}{k_2\beta}\frac{Q_{12}^2}{Q_{22}},$$

or, equivalently,

$$\gamma > \tilde{\gamma}_2 := \frac{1}{\lambda_{\min}(\tilde{\boldsymbol{D}})}\left(\frac{k_3^2}{k_2\beta}\frac{\lambda^2_{\max}(\tilde{\boldsymbol{D}})}{4\lambda_{\min}(\tilde{\boldsymbol{K}})} + k_4 k_M + k_3 k_C\right).$$

The thesis follows by defining $\tilde{\gamma} := \max\{\tilde{\gamma}_1;\ \tilde{\gamma}_2\}$ and applying again the Global Invariant Set theorem. □

Remark 2: In contrast to elastically decoupled soft robots, elastically dominated ones are stabilizable via simpler regulators since almost no knowledge of the dynamic parameters is needed, and only the actuated variables must be measured. However, both controllers do not require the robot stiffness because they learn the static elastic forces during the task execution. As a result, these control laws are more robust with respect to those of [17], [18].

Remark 3: Thanks to the natural damping in the dynamics, the controllers (5) and (10) do not need the derivative action, i.e., $\boldsymbol{K}_D$ can be set to zero. However, even if it does not affect stability, the damping injection may play a fundamental role in the closed-loop performance.

Remark 4: The proposed control laws stabilize the dynamics also under fully actuated approximations, i.e., when $m = n$.

V. Simulation Results

Here, we validate the results of Sections III and IV through extensive simulations on different planar soft robots moving in the vertical plane rotated so that the gravitational force yields a destabilizing effect on the dynamics. We model the robots under the piecewise constant curvature (PCC) assumption. A couple applied at its distal ends bends each actuated segment.

In all the simulations, the function $\boldsymbol{s}(\boldsymbol{x}) = \boldsymbol{s}_p(\boldsymbol{x}); p = 2$, is used for the integral action, which is initialized to zero, and the robot starts at rest in the straight configuration, i.e., $\boldsymbol{q}(0) = \boldsymbol{0}\,[\mathrm{rad}]$ and $\dot{\boldsymbol{q}}(0) = \boldsymbol{0}\,[\mathrm{rad/s}]$.

See the multimedia material for a video of the simulations.

A. Simulation 1 (Elastically Decoupled and Dominated)

Consider a planar soft robot with two actuated segments, each discretized into four CC segments. Consequently, the actuation matrix takes the form [7]

$$\boldsymbol{A} = \begin{pmatrix} 1 & 1 & 1 & 1 & 0 & 0 & 0 & 0 \\ 0 & 0 & 0 & 0 & 1 & 1 & 1 & 1 \end{pmatrix}^T,$$

and the two actuated variables can be chosen as the sum of the curvatures of each actuated segment, i.e., $q_{a,1} = \theta_1 + \theta_2 + \theta_3 + \theta_4$ and $q_{a,2} = \theta_5 + \theta_6 + \theta_7 + \theta_8$. As a result, $\boldsymbol{q}_a$ is the attitude of the tip of the actuated segments. The six unactuated coordinates are taken as elements of the null space of $\boldsymbol{A}$, i.e., $\boldsymbol{q}_u \in \ker \boldsymbol{A}$.

Each CC segment has mass $m_i = 0.05\,[\mathrm{kg}]$, length $l_i = 0.04\,[\mathrm{m}]$, and uniformly distributed stiffness and damping $\boldsymbol{K}_{\boldsymbol{\theta}} = 0.8 \cdot \boldsymbol{I}_8\,[\mathrm{Nm/rad}]$ and $\boldsymbol{D}_{\boldsymbol{\theta}} = 0.01 \cdot \boldsymbol{I}_8[\mathrm{Nms/rad}]; i \in \{1, \ldots, 8\}$. The control gains are taken as $\boldsymbol{K}_P = \mathrm{diag}\{1.5,\ 1.3\}[\mathrm{Nm/rad}]$, $\boldsymbol{K}_D = \mathrm{diag}\{0.3,\ 0.1\}[\mathrm{Nms/rad}]$, $\boldsymbol{K}_I = 0.5 \cdot \boldsymbol{I}_2[\mathrm{Nm/rads}]$ and $\gamma = 2$, respectively.

Being $\boldsymbol{K}_{\boldsymbol{\theta}}$ diagonal and large enough, the robot is elastically decoupled and dominated. As a consequence, both the P-satI-D+ (5) and P-satI-D (10) control laws can be used. The reference for the actuated variables is (in [rad])

$$\boldsymbol{q}_{a,d} = \begin{cases} \begin{pmatrix} -\frac{\pi}{3} & \frac{\pi}{3} \end{pmatrix}^T; & t \in [0; 7)\,[\mathrm{s}] \\ \begin{pmatrix} \frac{\pi}{2} & -\frac{\pi}{4} \end{pmatrix}^T; & t \in [7; 14]\,[\mathrm{s}] \end{cases}, \tag{16}$$

which results in the overall desired configuration

$$\boldsymbol{q}_d = \begin{cases} \boldsymbol{q}_{d,1}; & t \in [0; 7)\,[\mathrm{s}] \\ \boldsymbol{q}_{d,2}; & t \in [7; 14]\,[\mathrm{s}] \end{cases}, \tag{17}$$

with

$$\boldsymbol{q}_{d,1} = \begin{pmatrix} -\frac{\pi}{3} & \frac{\pi}{3} & 0.13 & 0.21 & -0.07 & -0.02 & 0.01 & 0.03 \end{pmatrix}^T,$$

$$\boldsymbol{q}_{d,2} = \begin{pmatrix} \frac{\pi}{2} & -\frac{\pi}{4} & 0.15 & 0.22 & -0.04 & -0.02 & 0 & 0 \end{pmatrix}^T.$$

Figs. 2(a) and (d) report the time evolution of the configuration variables under the P-satI-D+ and the P-satI-D, respectively. Both controllers impose, as expected, the desired configuration; however, the P-satI-D+ performs better than the P-satI-D. Indeed, the former yields slightly smaller overshoots compared to the latter. The P-satI-D+ learns only the static elastic forces at $\boldsymbol{q}_d$, whereas the P-satI-D also the gravitational torques. Consequently, the integral of the P-satI-D accumulates a larger error, resulting in higher peaks at the beginning of each motion. Note that the performance of the P-satI-D could be improved by providing an estimate of $\boldsymbol{G}_a(\boldsymbol{q}_d)$, if available. Figs. 2(b) and (e) report the time evolution of the control torques, where no notable difference occurs. Furthermore, stroboscopic views of the resulting robot motions are depicted in Figs. 2(f) and (c).

B. Simulation 2 (Elastically Decoupled)

Consider a planar cylindrical-shaped soft actuator made of isotropic material discretized into four CC segments with length $l_i = 0.05\,[\mathrm{m}]$ and mass $m_i = 0.05\,[\mathrm{kg}]; i \in \{1, \ldots, 4\}$. Stiffness and damping are uniformly distributed, and equal to $\boldsymbol{K}_{\boldsymbol{\theta}} = 0.005 \cdot \boldsymbol{I}_4\,[\mathrm{Nm/rad}]$ and $\boldsymbol{D}_{\boldsymbol{\theta}} = 0.0025 \cdot \boldsymbol{I}_4[\mathrm{Nm/rads}]$, respectively. As a consequence the robot is elastically decoupled and (5) can be used to regulate $q_a = \theta_1 + \theta_2 + \theta_3 + \theta_4$. The reference configuration for the actuated variable is (in [rad])

$$q_{a,d} = \begin{cases} \frac{\pi}{2}; & t \in [0; 7)\,[\mathrm{s}] \\ -\frac{\pi}{3}; & t \in [7; 14]\,[\mathrm{s}] \end{cases}. \tag{18}$$

In addition, an external disturbance $d = 0.2\,[\mathrm{Nm}]$ acts starting from $8\,[\mathrm{s}]$. The control gains are taken as $K_P = 0.75\,[\mathrm{Nm/rad}]$, $K_D = 0.03\,[\mathrm{Nms/rad}]$, $K_I = 0.5\,[\mathrm{Nm/rads}]$ and $\gamma = 2$.

Fig. 3(a) shows the time evolution of the configuration variables. The actuated variable quickly converges to the desired value, while the unactuated ones remain bounded and reach an equilibrium point. As expected, the $\boldsymbol{q}_u$ variables oscillate significantly because we do not have direct control authority over them. Furthermore, the Coriolis and centrifugal forces couple the evolution of $\boldsymbol{q}_u$ with q_a. Since the regulator does not perform any unnecessary cancellation of model terms for stability, the evolution of $\boldsymbol{q}_u$, which mainly depends on the

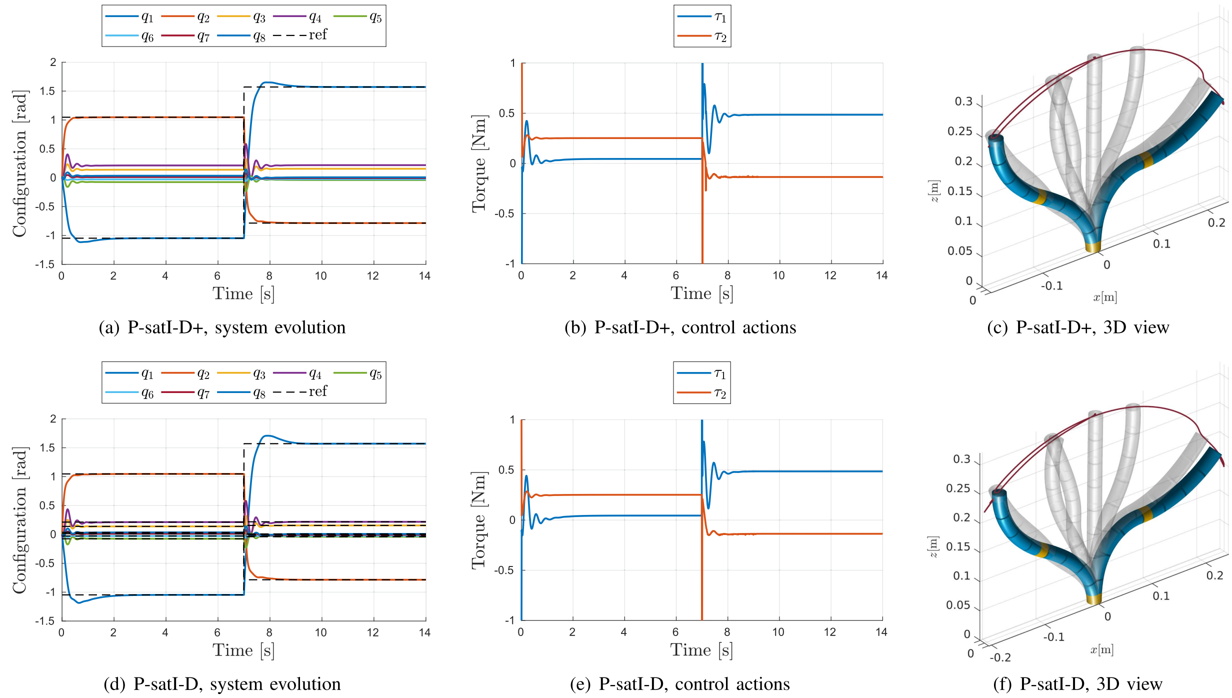

(a) P-satI-D+, system evolution (b) P-satI-D+, control actions (c) P-satI-D+, 3D view

(d) P-satI-D, system evolution (e) P-satI-D, control actions (f) P-satI-D, 3D view

Fig. 2. Simulation 1 (Elastically decoupled and dominated). Time evolution of the closed-loop configuration variables under (a) the P-satI-D+ (5) and (d) the P-satI-D (10) for reference (17). The output of the two controllers is shown in (b) and (e). Furthermore, (c) and (f) present stroboscopic views of the robot motion in the workspace under the P-satI-D+ and (b) the P-satI-D, respectively. The steady-state configurations are depicted in blue, while the transient ones are in gray. A red line shows the tip trajectory. A dark yellow stripe represents the hinge between two consecutive actuated segments.

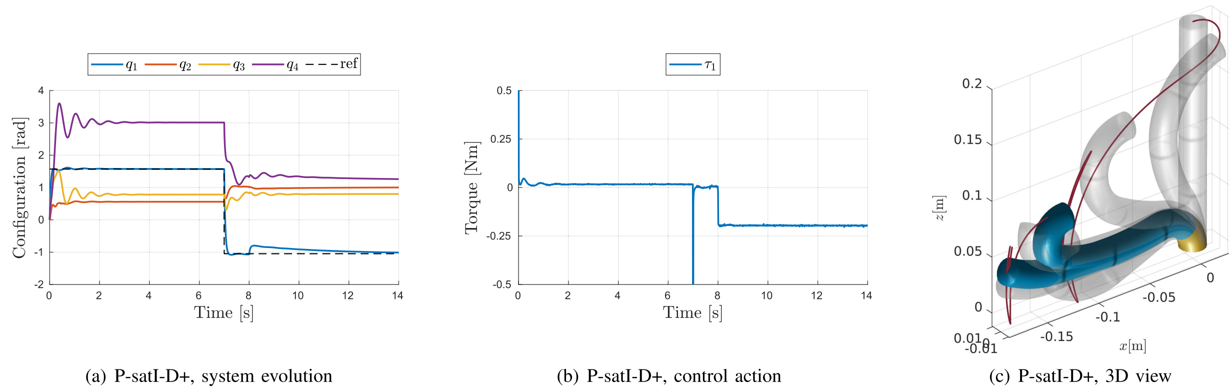

(a) P-satI-D+, system evolution (b) P-satI-D+, control action (c) P-satI-D+, 3D view

Fig. 3. Simulation 2 (Elastically decoupled). Time evolution of the configuration variables (a) and of the control effort (b) under the P-satI-D+ for reference (18). (c) A stroboscopic view of the robot motion in its workspace organized as Fig. 2.

system damping, may also affect q_a. The control torque, shown in Fig. 3(b), increases in magnitude as soon as d appears, and the integral action quickly compensates for the external disturbance. Because of the excessive weight, the actuator collapses, and the task is accomplished by moving mainly the tip, as it appears from the stroboscopic plot of the robot in Fig. 3(c).

C. Simulation 3 (Elastically Dominated)

Finally, consider a conical-shaped tentacle of isotropic material. The robot is modeled through four CC segments with length $l_i = 0.05\,[\mathrm{m}];\ i \in \{1,\ldots,4\}$. The segment masses are $m_{\{1,2,3,4\}} = \{0.05,\ 0.04,\ 0.03,\ 0.02\}\,[\mathrm{kg}]$, whereas stiffness and damping are, respectively,

$$\boldsymbol{K_\theta} = \mathrm{diag}\{0.1; 0.13; 0.16; 0.2\}\,[\mathrm{Nm/rad}]$$

and

$$\boldsymbol{D_\theta} = \mathrm{diag}\{0.03; 0.0036; 0.043; 0.05\}\,[\mathrm{Nms/rad}].$$

Differently from the previous simulation, we choose $K_P = 0.3\,[\mathrm{Nm/rad}]$ and $K_I = 0.6\,[\mathrm{Nm/rads}]$. Being the stiffness large enough, the potential field is convex and the robot is elastically dominated with again $q_a = \theta_1 + \theta_2 + \theta_3 + \theta_4$. Thus, the P-satI-D law (10) can be used to regulate q_a, for which the commanded target (in [rad])

$$q_{a,d} = \begin{cases} -\pi; & t \in [0;7)\,[\mathrm{s}] \\ \frac{\pi}{2}; & t \in [7;14]\,[\mathrm{s}] \end{cases}, \tag{19}$$

results in the reference configuration

$$\boldsymbol{q}_d = \begin{cases} [-\pi\ 0.14\ 0.26\ 0.33]; & t \in [0;7)\,[\mathrm{s}] \\ [\ \ \frac{\pi}{2}\ 0.07\ 0.07\ 0.02]; & t \in [7;14]\,[\mathrm{s}] \end{cases}. \tag{20}$$

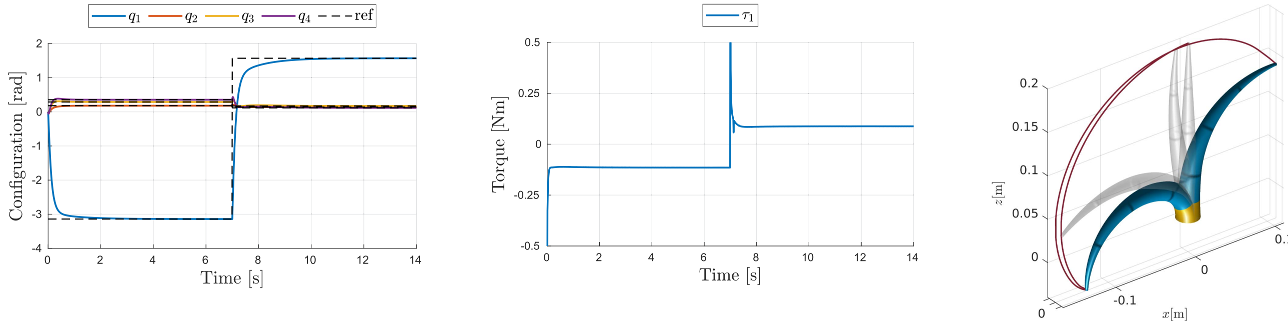

(a) P-satI-D, system evolution (b) P-satI-D, control action (c) P-satI-D, 3D view

Fig. 4. Simulation 3 (Elastically dominated). Time evolution of the configuration variables (a) and of the control effort (b) under the P-satI-D for reference (20). (c) A stroboscopic view of the robot motion in its workspace organized as Fig. 2.

Figs. 4(a) and (b) illustrate the closed-loop evolution of the configuration variables and of the control input, respectively. As expected, $\boldsymbol{q}$ converges to the desired set point. Since the elastic forces support the arm against gravity, the curvatures attain similar values, and the robot no longer collapses, in contrast to Simulation 2. This fact can also be seen in Fig. 4(c), which illustrates the robot motion.

VI. Conclusions and Future Work

In this letter, we proposed new classes of controllers for elastically decoupled and elastically dominated soft robots. For the former, the actuated variables can be regulated to any desired target configuration through a PID with saturated integral action and with gravity cancellation. Along the same line of thought, elastically dominated soft robots can be globally asymptotically stabilized using a simple PID controller with saturated integral action. The integral yields two benefits: (i) it does remove from the control law a term that accounts for the elastic forces, and (ii) it makes the closed-loop robust with respect to matched constant disturbances. Finally, the theoretical results have been verified through extensive simulations. Future work will be devoted to the experimental validation of these controllers, and to the study of tuning techniques for the proposed regulators.

References

[1] C. Della Santina, M. G. Catalano, and A. Bicchi, “Soft robots,” in *Encyclopedia of Robotics*, M. Ang, O. Khatib, and B. Siciliano, Eds., Berlin/Heidelberg, Germany: Springer, 2020, pp. 1–15.

[2] S. Aracri et al., “Soft robots for ocean exploration and offshore operations: A perspective,” *Soft Robot.*, vol. 8, no. 6, pp. 625–639, 2021.

[3] D. Cafolla, M. Russo, and G. Carbone, “CUBE, a cable-driven device for limb rehabilitation,” *J. Bionic Eng.*, vol. 16, no. 3, pp. 492–502, 2019.

[4] S. Grazioso, G. Di Gironimo, and B. Siciliano, “A geometrically exact model for soft continuum robots: The finite element deformation space formulation,” *Soft Robot.*, vol. 6, no. 6, pp. 790–811, 2019.

[5] M. Dubied, M. Y. Michelis, A. Spielberg, and R. K. Katzschmann, “Sim-to-real for soft robots using differentiable FEM: Recipes for meshing, damping, and actuation,” *IEEE Robot. Automat. Lett.*, vol. 7, no. 2, pp. 5015–5022, Apr. 2022.

[6] F. Renda, F. Boyer, J. Dias, and L. Seneviratne, “Discrete Cosserat approach for multisection soft manipulator dynamics,” *IEEE Trans. Robot.*, vol. 34, no. 6, pp. 1518–1533, Dec. 2018.

[7] C. Della Santina, C. Duriez, and D. Rus, “Model based control of soft robots: A survey of the state of the art and open challenges,” 2021, *arXiv:2110.01358*.

[8] B. Caasenbrood, A. Pogromsky, and H. Nijmeijer, “Control-oriented models for hyperelastic soft robots through differential geometry of curves,” *Soft Robot.*, 2022.

[9] E. Franco, T. Ayatullah, A. Sugiharto, A. Garriga-Casanovas, and V. Virdyawan, “Nonlinear energy-based control of soft continuum pneumatic manipulators,” *Nonlinear Dyn.*, vol. 106, no. 1, pp. 229–253, 2021.

[10] M. Thieffry, A. Kruszewski, T.-M. Guerra, and C. Duriez, “Trajectory tracking control design for large-scale linear dynamical systems with applications to soft robotics,” *IEEE Trans. Control Syst. Technol.*, vol. 29, no. 2, pp. 556–566, Mar. 2021.

[11] C. Della Santina, “The soft inverted pendulum with affine curvature,” in *Proc. IEEE 59th Conf. Decis. Control*, 2020, pp. 4135–4142.

[12] E. Franco and A. Garriga-Casanovas, “Energy-shaping control of soft continuum manipulators with in-plane disturbances,” *Int. J. Robot. Res.*, vol. 40, no. 1, pp. 236–255, 2021.

[13] E. Franco, A. Garriga-Casanovas, and A. Donaire, “Energy shaping control with integral action for soft continuum manipulators,” *Mechanism Mach. Theory*, vol. 158, 2021, Art. no. 104250.

[14] A. H. Khan, Z. Shao, S. Li, Q. Wang, and N. Guan, “Which is the best PID variant for pneumatic soft robots? An experimental study,” *IEEE/CAA J. Automatica Sinica*, vol. 7, no. 2, pp. 451–460, Mar. 2022.

[15] P. Huang, J. Wu, C.-Y. Su, and Y. Wang, “Tracking control of soft dielectric elastomer actuator based on nonlinear PID controller,” *Int. J. Control*, pp. 1–11, 2022.

[16] A. F. Alifdhyatra, B. A. Y. Sunarya, E. M. I. Hidayat, I. Anshori, and Y. W. Hadi, “Development of pneumatic networks soft robot with anti-windup PID control,” in *Proc. IEEE 13th Control Syst. Graduate Res. Colloq.*, pp. 25–30, 2022.

[17] P. Pustina, C. Della Santina, and A. De Luca, “Feedback regulation of elastically decoupled underactuated soft robots,” *IEEE Robot. Automat. Lett.*, vol. 7, no. 2, pp. 4512–4519, Apr. 2022.

[18] P. Borja, A. Dabiri, and C. Della Santina, “Energy-based shape regulation of soft robots with unactuated dynamics dominated by elasticity,” in *Proc. IEEE 5th Int. Conf. Soft Robot.*, 2022, pp. 396–402.

[19] P. Borja, C. Della Santina, and A. Dabiri, “On the role of coupled damping and gyroscopic forces in the stability and performance of mechanical systems,” *IEEE Control Syst. Lett.*, vol. 6, pp. 3433–3438, 2022.

[20] B. Siciliano, L. Sciavicco, L. Villani, and G. Oriolo, *Robotics*. London, U.K.: Springer, 2009.

[21] R. Kelly, “Global positioning of robot manipulators via PD control plus a class of nonlinear integral actions,” *IEEE Trans. Autom. Control*, vol. 43, no. 7, pp. 934–938, Jul. 1998.

[22] R. A. Horn and C. R. Johnson, *Matrix Analysis*. Cambridge, U.K.: Cambridge Univ. Press, 2012.

[23] V. Santibañez, R. Kelly, A. Zavala–Rio, and P. Parada, “A new saturated nonlinear PID global regulator for robot manipulators,” *IFAC Proc. Volumes*, vol. 41, no. 2, pp. 11690–11695, 2008.

[24] J.-J. E. Slotine and W. Li, *Applied Nonlinear Control*. Hoboken, NJ, USA: Prentice Hall, 1991.

[25] R. Abraham, J. E. Marsden, and T. Ratiu, *Manifolds, Tensor Analysis, and Applications*. Berlin/Heidelberg, Germany: Springer, 2012.

Open Access provided by ‘Università degli Studi di Roma “Tor Vergata”’ within the CRUI CARE Agreement